Envelope functions for a three-band semiconductor in a uniform electric field

R. Beresford
Division of Engineering, Brown University, Box D, Providence, Rhode Island 02912
(Received 10 January 1994; revised manuscript received 14 February 1994)

The three-band effective Hamiltonian of $\mathbf{k}\cdot\mathbf{p}$ perturbation theory, which is relevant for nonparabolic semiconductor conduction bands, is solved for the case of a uniform electric field along the heterostructure growth axis. The solutions are analytical and nearly exact, typically giving conduction-band eigenvalues to accuracies within a fraction of a percent. Good accuracy is obtained by considering the effects of the split-off hole band via an effective two-band interaction, which is obtained by linearizing the valence-band term in the exact two-band subspace of the three-band Hamiltonian. A straightforward extension provides an approximate analytical account of the remote band perturbations as well. The solutions are based on exact analytical results for the two-band model (electrons and light holes only), from which a universal family of curves characterizing the subband shift versus electric field has been derived. As a test case of the approximate three-band solution, the quantum-well Stark shift of the conduction electron is computed and compared with exact numerical results.

INTRODUCTION

Analysis of semiconductor heterostructures with abrupt transitions from one material to another is profitably carried out by the envelope-function-approximation method. Many incisive examples may be found in the book by Bastard[1] and references therein. As originally conceived, the effective-mass approach requires that the external potentials be slowly varying in space, and this requirement is never met in modern heterostructures. However, more recently it has been recognized that the envelope-function approximation can be rigorously justified when the envelopes themselves are slowly varying,[2] and this condition is easily met. However, there is the important proviso that all relevant bands be included in the envelope-function calculation. In $GaAs/Al_xGa_{1-x}As$ structures it is frequently possible to consider only the conduction band at the zone center. In contrast, in the interesting case of the InAs/(Al,Ga)Sb material system, the conduction-band minimum of InAs and the valence-band maximum of $Al_xGa_{1-x}Sb$ come near each other or even overlap, so that strong interband coupling is observed.[3] For these and similar situations, the following contribution shows analytically how to obtain approximate (but quite accurate) envelope functions for three interacting bands—conduction, light hole, and split-off hole—in the presence of a uniform external electric field. These solutions are useful in analyzing interband tunneling experiments and quantum confinement effects in narrow-band-gap materials. As a sample application, the contributions to the Stark shift in an infinite quantum well arising from the light- and spin-split-hole bands are computed.

In a previous report, we gave envelope-function solutions for a model system consisting of a symmetric two-band semiconductor in a uniform electric field.[4] Since these solutions are the basis for the present three-band analysis, a very brief restatement of these prior results is necessary. The method of solution proceeds by analogy with the relativistic electron (Dirac equation), which is governed by mathematically identical relations. The model problem solved first is the one-dimensional Schrödinger equation for the two-band effective Hamiltonian of $\mathbf{k}\cdot\mathbf{p}$ perturbation theory:[5]

$$\begin{bmatrix} (\frac{1}{2}E_G - E - Fz) & -i\hbar v\dfrac{d}{dz} \\ -i\hbar v\dfrac{d}{dz} & (-\frac{1}{2}E_G - E - Fz) \end{bmatrix} \begin{bmatrix} f_c \\ f_v \end{bmatrix} = 0 \ . \tag{1}$$

The position-dependent conduction-band edge is given by $E_C(z)=E_G/2-F(z-z_0)$, where we are taking the midgap as the energy zero point $[E_V(z)=E_C(z)-E_G]$. The constant Fz_0 is arbitrary and may take any convenient value, such as zero. The free-electron kinetic-energy term is for the time being ignored, and in any case will be small in comparison to these terms when this two-band model is itself applicable. The z axis is the growth axis, and the electric force along this direction is represented as F. The velocity v is that associated with Kane's momentum matrix element p.[6] System (1) can be solved in terms of parabolic cylinder functions,[7] by making a change of parameters according to

$$x \equiv \left[\frac{2}{i\hbar vF}\right]^{1/2}(E+Fz) \ , \quad \mu \equiv \frac{\frac{1}{4}E_G^2}{2\hbar vF} \ . \tag{2}$$

Then the envelope functions are

$$\begin{aligned} f_c(x) &= A\left\{D_{-i\mu}(x) + \left[\frac{\mu}{i}\right]^{1/2} D_{-1-i\mu}(x)\right\} \\ &\quad + B\left\{D_{-i\mu}(-x) - \left[\frac{\mu}{i}\right]^{1/2} D_{-1-i\mu}(-x)\right\} , \\ f_v(x) &= A\left\{D_{-i\mu}(x) - \left[\frac{\mu}{i}\right]^{1/2} D_{-1-i\mu}(x)\right\} \\ &\quad + B\left\{D_{-i\mu}(-x) + \left[\frac{\mu}{i}\right]^{1/2} D_{-1-i\mu}(-x)\right\} . \end{aligned} \tag{3}$$

A and B are the constants dictated by the boundary conditions. Note that if the sign of x is changed in these expressions, the signs of the terms involving $D_{-1-i\mu}$ also must be changed. The result therefore is simply an exchange of the constants A and B. Changing the sign of x amounts to changing the signs of E and z, and since the sign of dE/dk is unchanged in this operation, $f_c(-x)$ represents a carrier in the lower band, while $f_v(-x)$ represents a carrier in the upper band. An asymptotic analysis of the fundamental solutions indicates that the A term contributes only a positive-going wave, but the B term has both positive- and negative-going parts. To obtain (asymptotically) a purely negative-going wave requires $A+e^{\pi\mu}B=0$.

As an application of the foregoing results, consider the eigenvalue equation for a quantum well confined by infinitely high barriers. In the one-band case, it is of some value to note that the eigenvalues when normalized to the confinement energy

$$E_a \equiv \frac{\hbar^2\pi^2}{2m^*a^2} \tag{4}$$

are a function only of the normalized field, Fa/E_a (Ref. 8). Therefore, a single plot of subband shift versus field universally characterizes any quantum well via rescaling. In the two-band model, however, there naturally arises a second parameter, namely the band-gap energy. It makes most sense to normalize all energies to half the band gap.

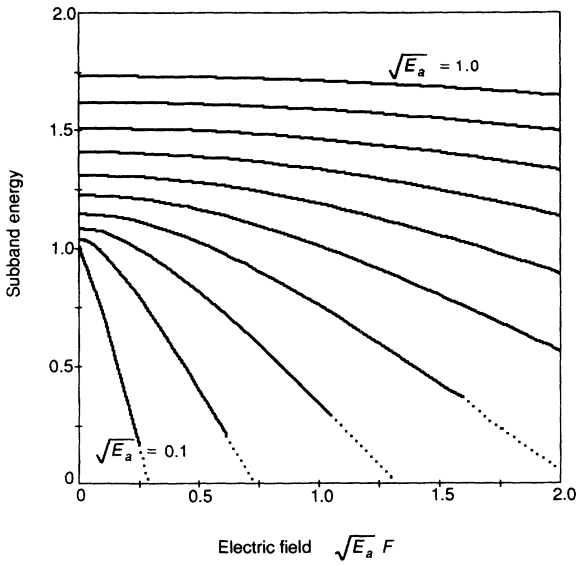

FIG. 1. The universal family of subband shifts vs electric field for the two-band model. The parameter $\sqrt{E_a}$, defined in Eq. (4) of the text, is the confinement energy for a well of width a in the one-band model. It is incremented in steps of 0.1 starting from the curve labeled 0.1 at the lower left. All energies are normalized to half the band gap; F represents the electric force times the well width; that is, the electrostatic potential energy difference across the well. The change to a dotted line in the lower four curves marks the point where the valence-band edge anticrosses the subband. This point is already well beyond the threshold for impact ionization (at F approximately equal to 3) and therefore is experimentally inaccessible.

Then the normalized subband energies are a function of two parameters (E_a and the product Fa):

$$\tilde{E}=\tilde{E}\left[\sqrt{\tilde{E}_a}\,,\sqrt{\tilde{E}_a}\tilde{F}\right],\quad \tilde{F}\equiv\frac{Fa}{\frac{1}{2}E_G}, \tag{5}$$

where the tildes represent normalization to half the band-gap energy. It now becomes possible to generate a universal family of subbands shifts, parametrized by the ratio of confinement energy to the band-gap energy. This family of curves is displayed in Fig. 1, in the form most convenient for considering the shifts as a function of the field strength. On the other hand, for a fixed field strength, the abscissa on this graph can represent a variation in the confinement energy, for example, by varying the well width. In this case, only one point on each curve is relevant, namely the point at the $\sqrt{E_a}$-axis value that corresponds to the $\sqrt{E_a}$ value on the curve. Note that the nominal threshold for impact ionization is $F=3E_G/2$, so that much higher fields are not experimentally realizable. In this two-band model, the valence-band edge shifts up with field and anticrosses the subbands shown at the points where the solid lines give way to dotted lines. This region of anticrossing also is beyond the experimentally accessible fields.

NEARLY EXACT ANALYTICAL SOLUTIONS FOR THREE BANDS

To generalize the model system (1), a finite spin-orbit splitting Δ should be included, as well as the coupling to the heavy-hole band that occurs for nonzero in-plane momentum. The present treatment considers nonzero Δ but no in-plane momentum. The main idea is to solve the three-band problem as an effective two-band problem, whose exact solutions are known from (3) above. For zero crystal momentum in the plane of the layers, the three-band model is essentially an exact account of the conduction electron, lacking only small remote-band-perturbation terms. To first order, the light and split-off holes each interact with the conduction electrons, but not with each other. Therefore, the conduction electron may be viewed as approximately interacting with an average valence-band state involving contributions from both light particle types. For any given energy, the effective interaction can be well modeled by a two-band form, and the present analysis applies.

Note that various effective two-band models can be conceived. For example, the dispersion relation in zero field can be approximated with a "best-fitting" two-band form. However, such an approximation mishandles certain dynamical effects that can be captured more accurately with the approach presented here. The better solution procedure is to project the three-band Hamiltonian onto a two-band subspace and then linearize the valence-band term. The relative magnitude of the remaining ignored terms may be estimated and lies in the range 1–10% for representative values of the parameters. Comparison of approximate and exact solutions shows that typically the error in eigenenergies is a fraction of a percent for conduction-band states.

The three-band effective Hamiltonian of $\mathbf{k}\cdot\mathbf{p}$ perturba-

tion theory is first reduced to an exact two-band form by introducing the valence-band envelope defined by

$$f_v(z)=\sqrt{\tfrac{2}{3}}f_{\rm lh}(z)-\sqrt{\tfrac{1}{3}}f_{\rm so}(z)\ , \tag{6}$$

where the subscripts lh and so refer to light holes and split-off holes, respectively. With this definition, the system (1) generalizes to

$$\begin{bmatrix} (\frac{1}{2}E_G-E-Fz) & -i\hbar v\dfrac{d}{dz} \\ -i\hbar v\dfrac{d}{dz} & (-\frac{1}{2}E_G-E-Fz)\delta(E+Fz) \end{bmatrix} \times \begin{bmatrix} f_c \\ f_v \end{bmatrix}=0\ , \tag{7}$$

the only new feature being the presence of the factor

$$\delta(E+Fz)\equiv 1+\left\{\frac{\frac{1}{3}\Delta}{\frac{1}{2}E_G+\frac{2}{3}\Delta+E+Fz}\right\}\ . \tag{8}$$

Considering energies from the valence-band edge and greater, this factor δ is never greater than $\frac{3}{2}$ nor less than 1. The limiting cases $\Delta\to 0$ and $\Delta\to\infty$ are subsumed in the previous exact analysis. The presence of this factor, however, apparently precludes an exact analytical solution.

An approximate solution may be obtained as follows. By means of a Taylor-series expansion around $(E+Fz)=0$ (the midgap at the origin of coordinates), the valence-band term in the effective Hamiltonian can be written as a polynomial in $(E+Fz)$, whose lowest-order terms are

$$(\tfrac{1}{2}E_G+E+Fz)\delta(E+Fz) \cong \tfrac{1}{2}E_G(1+u)+(E+Fz)(1+2u^2)+\cdots\ . \tag{9}$$

In this expression, the quantity u measures the strength of the spin-orbit interaction according to

$$u\equiv\left\{\frac{\frac{1}{3}\tilde{\Delta}}{1+\frac{2}{3}\tilde{\Delta}}\right\}\ , \tag{10}$$

and the tildes again indicate normalization with respect to half the band-gap energy. The magnitude of the ignored terms in expansion (9) increases as the band energy approaches $-(E_G/2+2\Delta/3)$, and this approximation scheme fails. However, for the interband tunneling experiments in III-V materials, the spin splitting is sizable and the approximation can be carried some way into the valence band. For example, if $\Delta=E_G$, then in normalized terms the ignored part is less than or about 0.2 for energies from -1.2 to $+2.4$ (the band edges lying at ± 1).

On introducing the transformation[9]

$$\begin{bmatrix} f_c \\ f_v \end{bmatrix}=\begin{bmatrix} (-\frac{1}{2}E_G-E-Fz)\delta(E+Fz) & i\hbar v\dfrac{d}{dz} \\ i\hbar v\dfrac{d}{dz} & (\frac{1}{2}E_G-E-Fz) \end{bmatrix} \times \begin{bmatrix} \Phi_c \\ \Phi_v \end{bmatrix}\ , \tag{11}$$

it is found that the functions Φ both satisfy the equation

$$\left\{\left[\hbar v\frac{d}{dz}\right]^2+\alpha(E+Fz)^2+\beta\tfrac{1}{2}E_G(E+Fz)+\gamma\tfrac{1}{4}E_G^2\right\}\Phi=0\ , \tag{12}$$

with the constants α, β, and γ calculated from

$$\begin{aligned} &\alpha=1+2u^2=1+u-(\tfrac{1}{3}\tilde{\Delta})^{-1}u^2\ , \\ &\beta=(\tfrac{1}{3}\tilde{\Delta})^{-1}u^2\ , \\ &\gamma=-(\alpha+\beta)\pm\frac{i\sqrt{\alpha}}{2\mu}\ . \end{aligned} \tag{13}$$

There are two equivalent versions of Eq. (12) depending on the sign chosen in the constant γ. Correspondingly, $\Phi_v=\pm\sqrt{\alpha}\Phi_c$. We make the latter choice (minus sign) for convenience and henceforth ignore this sign ambiguity. Equation (12) has two independent solutions in terms of the Weber functions $D_{-\sigma}(\pm X)$, provided

$$\begin{aligned} &x\equiv\left[\frac{2\sqrt{\alpha}}{i\hbar vF}\right]^{1/2}\left\{(E+Fz)+\tfrac{1}{2}E_G\frac{\beta}{2\alpha}\right\} \\ &\sigma\equiv i\mu\sqrt{\alpha}\left\{1+\frac{\beta}{\alpha}+\left[\frac{\beta}{2\alpha}\right]^2\right\}\ . \end{aligned} \tag{14}$$

It may be checked that these definitions simplify to the ones given in (2) when $\delta=1$ (that is, when $u=0$). Thus, by combining (13) and (14), an approximate analytical solution of the three band Hamiltonian is obtained:

$$\begin{aligned} f_c(x)&\cong\left[1-\frac{\beta}{2\alpha}\right]D_{-\sigma}(\pm x) \\ &\quad\mp\left[\frac{i}{\mu\sqrt{\alpha}}\right]^{1/2}\sigma D_{-1-\sigma}(\pm x)\ , \\ \sqrt{\alpha}f_v(x)&\cong\left[1+\frac{\beta}{2\alpha}\right]D_{-\sigma}(\pm x) \\ &\quad\pm\left[\frac{i\sqrt{\alpha}}{\mu}\right]^{1/2}\sigma D_{-1-\sigma}(\pm x)\ . \end{aligned} \tag{15}$$

As in (3), the alternative sign choices yield two independent solutions, which may be combined with arbitrary constant coefficients to yield the general solution.

To gain further insight into the nature of this approximate solution, compare definitions (2) and (14). The approximate three-band solution can be interpreted in terms of an effective confinement energy, an effective band gap, and a subband offset. In other words, take primed parameters defined by

$$\frac{E'_G}{E_G} \equiv \left[1+\frac{\beta}{\alpha}+\left[\frac{\beta}{2\alpha}\right]^2\right]^{1/2}, \quad \frac{E_a}{E'_a} \equiv \alpha \frac{E'_G}{E_G}, \tag{16}$$

and then solve a two-band problem using the primed parameters. According to (14), the approximately correct three-band eigenvalues are given by $E = E' - \Delta E$, where

$$\Delta E = \tfrac{1}{2} E_G \left[\frac{\beta}{2\alpha}\right](E_G/E'_G) . \tag{17}$$

Note that the normalized electric field differs in the primed system due to the changed energy normalization. When the situation of interest involves propagating states, the well width used in defining "confinement energy" amounts to arbitrary normalization of the spatial coordinate z. Neither this length nor an actual well width are scaled in going to the primed system. Rather, it is the factor $1/m^*$ representing the interband interaction that is considered to be rescaled in the primed system.

The variation with the spin splitting of the scale factors (16) and the offset in (17) are plotted in Fig. 2. It is of interest to compare these factors with an alternative purely "static" approximation obtained from the three-band dispersion relation in zero field. From (7) and (8), the zero-field dispersion relation is given implicitly by

$$(E^2 - \tfrac{1}{4}E_G^2)\delta(E) = (\hbar v k)^2 . \tag{18}$$

On expanding the left-hand side up to second order in E,

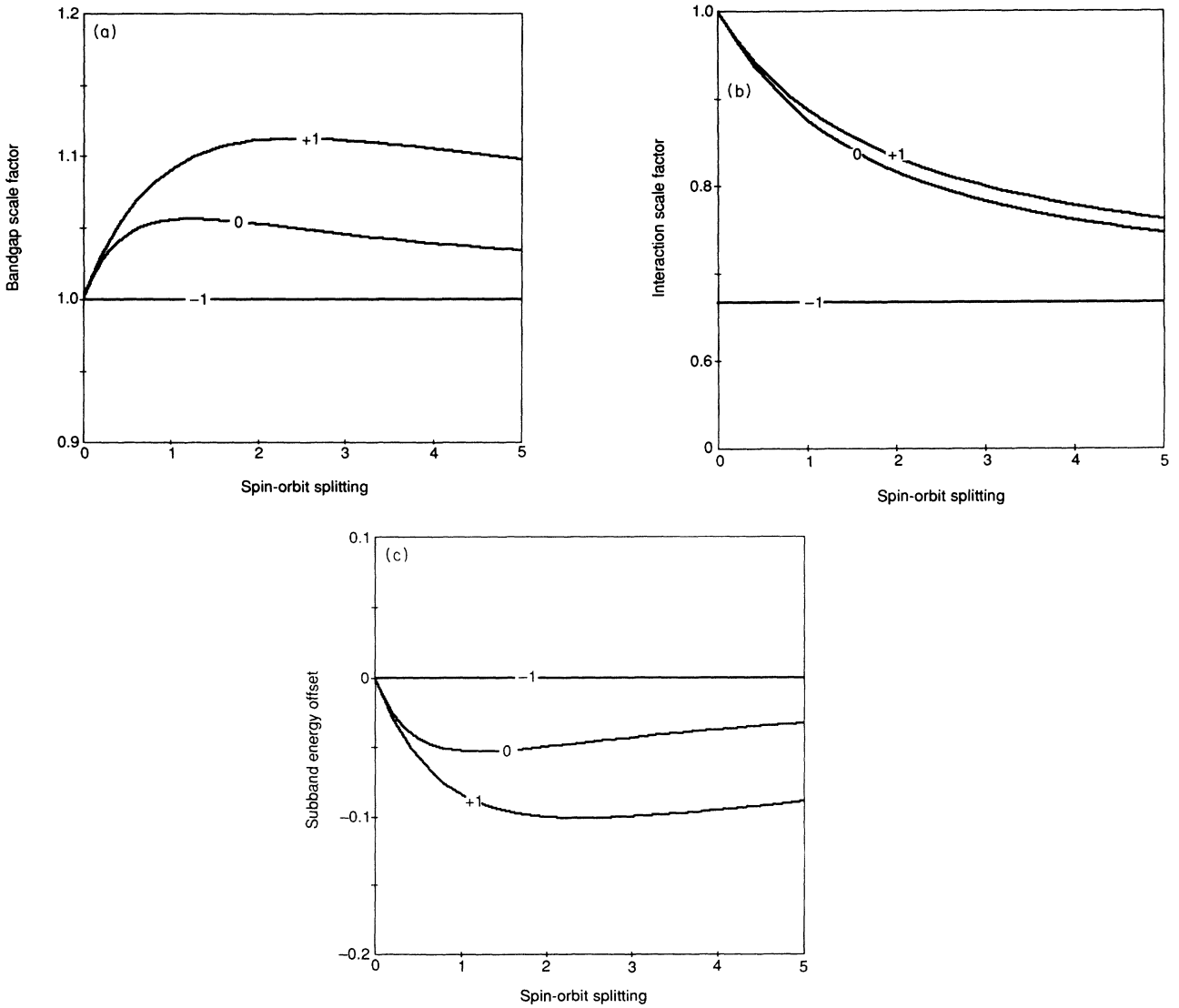

FIG. 2. Graphs showing the variation with the normalized spin-orbit splitting of the three factors used to model the split-off hole band effects. The effects are accounted for quite accurately by an effective two-band problem in which the band-gap energy (a) and the interaction (represented by the reciprocal effective mass) (b) are rescaled. In addition, the energy zero point is offset as shown in (c). All three quantities depend on the choice of expansion point, a fixed energy in or near the range of energies of interest in a given problem, around which the valence-band term of the effective Hamiltonian is linearized. In each case, three expansion points are shown for illustration, the valence-band edge (-1), the midgap (0), and the conduction-band edge ($+1$).

an effective two-band form can be extracted. The resulting approximation is found to be distinctly inferior to (16) and (17), the difference being that in this case neither band is treated exactly, whereas in the former case only the valence band is treated approximately. On the other hand, if both the conduction and light-hole bands are treated exactly and the split-off band factor is taken as approximately constant, $\delta=1+u$, the relations (13) and (16) are obtained with $\alpha=1+u$ and $\beta=0$. This approximation is again inferior, the interpretation being that the dynamical influence of the split-off hole band is ignored.

BAND-STRUCTURE INFLUENCE ON THE QUANTUM-CONFINED STARK EFFECT

The quality of the approximate three-band solution embodied in (15)–(17) is tested by computing the shift of the lowest subband energy versus electric field for a quantum well with infinitely high barriers. Exact numerical results are found to be higher than the approximate values found from (16), with the relative error ranging from fractions of a percent to a few percent, depending on the field strength and the size of the spin-orbit splitting. The good agreement between the exact and approximate results justifies the analysis of the conduction-band electron in the three-band model in terms of an effective two-band interaction.

As a starting point, consider the universal curve in Fig. 1 corresponding to $\sqrt{E_a}=0.6$ as the exact result for a three-band model with $\Delta\rightarrow 0$. In the limit $\Delta\rightarrow\infty$, a two-band system with $\sqrt{E_a}$ scaled by $\sqrt{(\frac{2}{3})}$ is obtained—that is, with $\sqrt{E_a}=0.4899$—and this case also may be computed exactly. The two curves that arise from these limiting cases (see Fig. 3) bracket all of the results for intermediate values of the spin-orbit splitting. The intermediate values shown ($\Delta=1$ and 5) are chosen for convenience and to approximately span the bracketed range.

The exact eigenvalues are determined by a relaxation algorithm,[10] using the approximate wave functions as an initial guess. The well width is divided into a mesh of equal size steps, and the envelope function values are obtained at the mesh points. The differential system (7) is replaced by a finite-difference system. Note that complex arithmetic is unnecessary if a relative phase of $\pi/2$ is factored out of one of the envelope functions. For each eigenvalue computation, three different sizes are tried (50, 100, and 200 steps). Extrapolation to the limit then gives the final estimate of the eigenvalue. To make a consistent comparison, the same relaxation code was used to compute the approximate eigenvalues by setting $\Delta=0$ and adjusting the parameters as specified in (16). Computations using Weber function evaluations from a commercial library[11] yielded essentially identical values for the approximate eigenvalues. For selected values of the field, a precise comparison of the exact and approximate results is

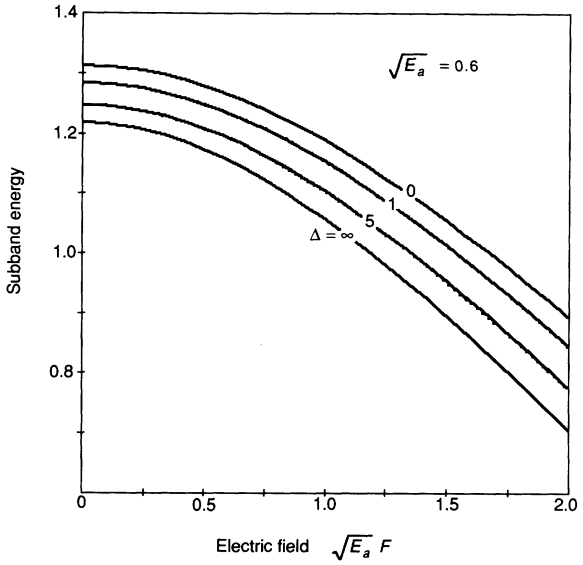

FIG. 3. Comparison of exact (solid) and approximate (dotted) computations of the subband energy shift vs field for several values of the spin-orbit splitting. The conduction-band edge is used for the expansion point in the approximate solution. The exact results come from a relaxation algorithm solution of the exact three-band effective Hamiltonian.

TABLE I. Comparison of exact and approximate eigenvalues for several values of the field and two values of the spin splitting. All energies are normalized to half the band gap. $E^{(0)}$: approximate value using the midgap ($E=0$) for the expansion point [see Eq. (25)]. $E^{(1)}$: approximate value using the conduction bnad edge ($E=1$) for the expansion point. $E^{[E(1)]}$: approximate value using $E^{(1)}$ as the expansion point (first iteration). Values in parentheses give the relative errors in percent.

	Δ=1				Δ=5			
$\sqrt{E_aF}$	$E^{(0)}$	$E^{(1)}$	$E^{[E(1)]}$	E_{exact}	$E^{(0)}$	$E^{(1)}$	$E^{[E(1)]}$	E_{exact}
0	1.278 93	1.283 23	1.283 32	1.283 32	1.240 62	1.246 60	1.246 76	1.246 76
	(−0.34)	(−0.0070)	(0.000)		(−0.49)	(−0.013)	(0.000)	
0.2	1.273 15	1.277 55	1.277 64	1.277 66	1.234 06	1.240 22	1.240 41	1.240 44
	(−0.35)	(−0.0085)	(−0.0013)		(−0.51)	(−0.017)	(−0.0028)	
0.5	1.243 57	1.248 47	1.248 58	1.248 67	1.200 71	1.207 79	1.208 05	1.208 29
	(−0.41)	(−0.016)	(−0.0068)		(−0.63)	(−0.041)	(−0.020)	
1.0	1.146 49	1.152 78	1.152 93	1.153 31	1.093 28	1.102 82	1.103 09	1.104 21
	(−0.59)	(−0.046)	(−0.033)		(−0.99)	(−0.13)	(−0.10)	
2.0	0.833 947	0.843 161	0.842 759	0.845 216	0.757 426	0.771 811	0.770 281	0.776 639
	(−1.3)	(−0.24)	(−0.29)		(−2.5)	(−0.62)	(−0.82)	

given in Table I. In most cases of interest, both the normalized field strength and the normalized spin splitting are around unity. In this range, the approximate solution is quite good, giving accuracies of a percent or better.

FURTHER DISCUSSION

Expansion (9) need not be carried out at $(E+Fz)=0$, but rather can be made around some point known to be closer to the energies of interest. For example, in transport problems, wave functions at a specified energy are desired, and this energy could serve as the basis for selecting an expansion point. In the computation just presented of the quantum-confined Stark effect, the energies of interest lie in the conduction band, so the conduction-band edge makes a sensible expansion point. In general, if one chooses $(E+Fz)=E_0$ as the expansion point, then u is to be redefined as

$$u \equiv \left\{ \frac{\frac{1}{3}\tilde{\Delta}}{1+\tilde{E}_0+\frac{2}{3}\tilde{\Delta}} \right\}, \tag{19}$$

and the parameters of (13) should be modified to

$$\beta=(\tfrac{1}{3}\tilde{\Delta})^{-1}u^2(1+\tilde{E}_0)^2 , \tag{20}$$

with the others remaining as before. If the value $E_0=E_G/2$ corresponding to the conduction-band edge is used to find the subband shifts, the results are substantially improved compared to using the midgap as the expansion point (see Table I). In the graph of Fig. 3, the dotted curves represent the results of this improved approximation and are barely distinguishable from the exact results at the resolution of the plots.

It might be thought that an even closer approximation could be obtained by iterating these results; that is, using the approximate eigenvalue as the expansion point and continuing until the result converges. This scheme was tried and the results of the first iteration are included in Table I as well (further iteration did not change the values shown). For smaller values of field and spin splitting, the iteration indeed improves the approximation, but once the eigenvalue falls below unity, the iteration moves the result the wrong way. Therefore, it is suggested that the simpler approach of a fixed expansion point in the energy region of interest gives a more practical solution. For the computations shown, the relative error never exceeds 1% under this approach, and this level of accuracy is considered more than adequate. Note also that when the conduction-band edge is used as the expansion point, the approximate subband energy shifts downward only, consistent with the correct behavior and with the approximate computation using the midgap as the expansion point.

Because the split-off band is treated nearly exactly, it becomes reasonable to consider whether the remote-band perturbations and, at the same level of correction, the free-electron kinetic energy can be accounted for, even if only approximately. For these purposes, the three-band effective Hamiltonian is augmented by diagonal terms of the form $\alpha_i k^2$, where $i=c$, lh, or so for the conduction, light-hole, and split-off-hole bands, respectively. These terms in principle are energy dependent, as they involve perturbation sums over remote bands. However, this energy dependence is safely neglected, on the grounds that the terms are small to begin with and the variation with energy is gradual. The values of the α_i are therefore fixed by requiring that the three-band dispersion relation produce the correct (experimental) effective masses m_i at the band edges. Since the three-band dispersion relation involves four parameters (the Kane matrix element as well as the α_i), one further condition is required, and for this one may use the sum rule $\alpha_c=\alpha_{\rm lh}+\alpha_{\rm so}$. Then it may be shown that

$$\begin{aligned} a_{\rm lh} &\equiv \alpha_{\rm lh}\tfrac{1}{2}E_G/(\hbar v)^2 = \left\{\frac{1+\tilde{\Delta}/3}{1+\tilde{\Delta}/2}\right\}\left\{\frac{1}{2}\left[1-\frac{1}{3+\tilde{\Delta}}\right]-\frac{m_{\rm lh}^{-1}}{m_c^{-1}+m_{\rm lh}^{-1}+m_{\rm so}^{-1}}\right\}, \\ a_{\rm so} &\equiv \alpha_{\rm so}\tfrac{1}{2}E_G/(\hbar v)^2 = \left\{\frac{1+\tilde{\Delta}/3}{1+\tilde{\Delta}/2}\right\}\left\{\frac{1}{2}\left[\frac{1}{3+\tilde{\Delta}}\right]-\frac{m_{\rm so}^{-1}}{m_c^{-1}+m_{\rm lh}^{-1}+m_{\rm so}^{-1}}\right\}, \end{aligned} \tag{21}$$

with a_c analogously defined and necessarily equal to $a_{\rm lh}+a_{\rm so}$. For InAs and GaSb as examples, the dimensionless a parameters are, in absolute value, on the order of 0.01–0.05. The velocity parameter is now

$$v=\left[\tfrac{1}{2}E_G\tfrac{1}{2}(m_c^{-1}+m_{\rm lh}^{-1}+m_{\rm so}^{-1})\left\{\frac{1+\tilde{\Delta}/2}{1+\tilde{\Delta}/3}\right\}\right]^{1/2}. \tag{22}$$

Proceeding as before, the Weber equation (12) is still approximately correct, provided the coefficient of the derivative operator is modified to be

$$\hbar v\left[1+a_c\left\{1+u+(1+2u^2)\tilde{E}_0\right\}+\left\{\tfrac{2}{3}a_{\rm lh}(1+u)^2+\tfrac{1}{3}a_{\rm so}(1-2u)^2\right\}(\tilde{E}_0-1)\right]^{1/2}. \tag{23}$$

In other words, to lowest order the remote-band effects are included simply as an effective v', that is, as a modification of the interband coupling.

As a test of this approximation, the problem treated above of the quantum-well Stark shift is computed again for the particular case of InAs, using the parameters $\sqrt{E_a}=0.6$, $\Delta=0.37$ eV, $m_c=m_{\rm lh}=0.023m_0$, and $m_{\rm so}=0.14m_0$. The results are displayed in Table II. For comparison, results for the same problem without considering the remote band perturbations are also shown. The conduction-band edge is used for the expansion point in the approximate solutions, and the relaxation code is used to find the exact eigenvalues. For the exact relaxation computations, the appropriate boundary conditions are that the conduction-band envelope and the derivatives of the light-hole and split-off-hole envelopes all vanish at both endpoints. That this condition is the correct one is checked by observing that as the field strength is reduced, the exact eigenvalues approach the zero-field value, which may be computed by iteration from the dispersion relation (18), modified to include the remote-band perturbation terms.

At zero field, inclusion of the remote-band perturbations lowers the exact eigenvalue by 1.9%. Approximation (23) produces a value only slightly different (+0.47%) from the exact result. At normalized field strength of unity, the remote-band terms lower the exact eigenvalue by 3.7%, but the approximation misses by −1.3%. In comparison, when the remote bands are removed from the problem entirely, the error in the approximate solution is only −0.091%. The difference is ascribed to the neglect of terms proportional to the product of the field and the first derivative of an envelope function. As the field increases, these terms eventually are comparable to the ones included in (23), which arise from the product of the energy and a second derivative. For weak or moderate fields, the approximation gives a good account of the remote-band perturbations.

TABLE II. Comparison of exact and approximate eigenvalues for several values of the field, with and without considering remote band perturbations. All energies are normalized to half the band gap. $E^{(1)}$: approximate value using the conduction band edge ($E=1$) for the expansion point. Values in parentheses give the relative errors in percent.

	$a_{\rm lh}=-0.050\,65$; $a_{\rm so}=+0.019\,11$		$a_{\rm lh}=a_{\rm so}=0$	
$\sqrt{E_aF}$	$E^{(1)}$	$E_{\rm exact}$	$E^{(1)}$	$E_{\rm exact}$
0	1.249 58 (+0.47)	1.243 79	1.267 09 (−0.011)	1.267 23
0.2	1.225 36 (−0.94)	1.237 02	1.261 14 (−0.014)	1.261 32
0.5	1.190 18 (−1.0)	1.202 63	1.230 74 (−0.031)	1.231 13
1.0	1.077 53 (−1.3)	1.091 97	1.131 36 (−0.091)	1.132 39
2.0	0.727 658 (−2.5)	0.746 686	0.812 930 (−0.46)	0.816 651

CONCLUSION

Realistic calculations of quantum-well Stark shifts have usually relied on numerical techniques. However, as shown here, quite accurate analytical approximations exist. The approximate solutions are physically motivated, deriving from the observation that the light particles of the valence band to first order interact only with the conduction band and not with each other. As a consequence, the conduction electron essentially feels a sort of composite or averaged valence-band state, which we have captured analytically by means of an effective two-band interaction and an effective band gap. For typical problems, the accuracy of this method is within a percent or so, making it an attractive alternative to numerical computation, particularly for rapid comparison with experimental results.

[1]G. Bastard, *Wave Mechanics Applied to Semiconductor Heterostructures* (Wiley, New York, 1988).
[2]M. G. Burt, J. Phys. Condens. Matter **4**, 6651 (1992).
[3]R. Beresford, L. F. Luo, and W. I. Wang, Semicond. Sci. Technol. **5**, S195 (1990).
[4]R. Beresford, Semicond. Sci. Technol. **8**, 1957 (1993).
[5]E. O. Kane and E. I. Blount, in *Tunneling Phenomena in Solids,* edited by E. Burstein and S. Lundqvist (Plenum, New York, 1969).
[6]E. O. Kane, J. Phys. Chem. Solids **12**, 181 (1959).
[7]J. C. P. Miller, in *Handbook of Mathematical Functions,* edited by M. Abramowitz and I. A. Stegun (Dover, New York, 1972).
[8]D. A. B. Miller, D. S. Chemla, T. C. Damen, A. C. Gossard, W. Wiegmann, T. H. Wood, and C. A. Burrus, Phys. Rev. B **32**, 1043 (1985).
[9]R. P. Feynman and M. Gell-Mann, Phys. Rev. **109**, 193 (1958).
[10]W. H. Press, B. P. Flannery, S. A. Teukolsky, and W. T. Vetterling, *Numerical Recipes in Pascal: The Art of Scientific Computing* (Cambridge University Press, Cambridge, 1989), pp. 645–657. Many ideas of the relaxation code are credited to P. P. Eggleton, *Monthly Notices of the Royal Astronomical Soc.* **151**, 351 (1971).
[11]S. Wolfram, *Mathematica* (Addison-Wesley, Redwood City, CA, 1991), pp. 570ff. The parabolic cylinder functions are related to Whittaker functions which are related to confluent hypergeometric (Kummer) functions, which may be evaluated for arbitrary arguments. However, large imaginary values of the parameters should be avoided.